



Supplementary Information for

**Essential role for autophagy protein ATG7 in the maintenance of intestinal stem cell  
integrity**

Coralie Trentesaux<sup>1</sup>, Marie Fraudeau<sup>1</sup>, Caterina Luana Pitasi<sup>1</sup>, Julie Lemarchand<sup>1</sup>, Sébastien Jacques<sup>1</sup>, Angéline Duche<sup>1</sup>, Franck Letourneur<sup>1</sup>, Emmanuelle Naser<sup>1</sup>, Karine Bailly<sup>1</sup>, Alain Schmitt<sup>1</sup>, Christine Perret<sup>1</sup>, Béatrice Romagnolo<sup>\*1</sup>

\* Corresponding author : Béatrice Romagnolo  
Email: [beatrice.romagnolo@inserm.fr](mailto:beatrice.romagnolo@inserm.fr)

**This PDF file includes:**

Supplementary text  
Figures S1 to S7  
Tables S1  
SI References

## Supplementary Information Materials and Methods

### Immunostaining and *in situ* hybridization

Immediately after death, the entire gastrointestinal tract of the mouse was removed, splayed open along its length and rolled up from the proximal to the distal end to form a 'Swiss roll'. Tissues were fixed by incubation in 4% paraformaldehyde overnight at 4°C and embedded in paraffin wax. Sections (3 µm thick) were cut and stained with hematoxylin and eosin. Immunohistochemistry was performed as previously described (1). We treated 5 µm sections with 3% hydrogen peroxide for 15 min at room temperature. For both immunohistochemistry and immunofluorescence, antigens were retrieved by boiling for 15 min in citrate buffer (10 mM, pH 6) or for 40 min in Tris-EDTA buffer (100 mM Tris, 12.6 mM, pH 9) for γH2AX in a microwave pressure cooker (EZ retriever, Biogenex). For BrdU staining, DNA was denatured in 2.5 N HCl for 30 min. Sections were incubated in blocking solution (2% goat serum, 1% BSA in TBST) for 20 min at room temperature. For mouse primary antibodies, the Vector M.O.M. kit was used. The sections were then incubated overnight at 4°C with primary antibodies diluted in blocking solution. Primary antibodies targeting the following proteins were used: p62 (Enzo, BML-PW9860-0100, 1:200), ubiquitin (MBL, MK 11-3, 1:200), cleaved caspase-3 (Cell Signaling, 9661S, 1:200), p53 (Leica, NCL-p53-CM5p, 1:200), lysozyme (Dako, EC.3.2.1.17, 1:200), BrdU (Abcam, ab6326, 1:500), Olfm4 (Cell Signaling, CS 39141S, 1:400), γH2AX (Millipore, 05-636, 1:300), GFP (Abcam, ab13970, 1:200), and LC3 (Enzo, ALX-803-080-C100). Specific binding was detected with a biotinylated secondary antibody and ABC reagent (Vector) for immunohistochemistry, and the signal was developed with DAB (Vector). Hematoxylin was used for the counterstaining of nuclei. For immunofluorescence, Alexa Fluor-coupled secondary antibodies (Thermo Fisher Scientific) were used, Hoechst stain was used for the counterstaining of nuclei, and slides were mounted in Vectashield fluorescence mounting medium (Vector). Slides were then imaged with an Olympus BX63F wide-field microscope or a Yokogawa CSU-X1 Spinning Disk (Yokogawa, Tokyo, Japan) coupled with a Leica DMI6000B microscope (Leica Microsystems GmbH, Wetzlar, Germany). Images were acquired with MetaMorph 7 software. Apoptosis was analyzed with a TUNEL assay kit, according to the manufacturer's instructions (Calbiochem, QIA33 for visible staining, Promega, G3250 for

fluorescent labeling). *In situ* hybridization was performed as previously described (2). Plasmids containing the *Olfm4* cDNA sequences (gift from H. Clevers, Hubrecht Institute for Developmental Biology and Stem Cell Research and University Medical Centre Utrecht, Utrecht, Netherlands) were used for the generation of cRNA probes.

### **Crypt isolation and organoid culture**

Crypts were isolated and cultured as previously described (3). Briefly, intestines were opened longitudinally, washed with cold PBS, and incubated in 15 mM EDTA in PBS for 25 minutes on ice. The tissue was then removed from the EDTA and vigorously vortexed in multiple fractions to release crypts. Fractions enriched in crypts were passed through a cell strainer with 70- $\mu$ m pores (BD Bioscience) to remove residual villi. For organoid culture, isolated crypts were counted and pelleted. We mixed 500 crypts with 50  $\mu$ l growth factor-reduced Matrigel (Corning), which was then plated on 24-well plates with 500  $\mu$ l advanced DMEM/F12 (Invitrogen) containing the following growth factors: EGF (Peprotech); R-spondin 1 (R&D Systems); and noggin (Peprotech). The growth medium was also supplemented with N2 and B27 (Invitrogen). The organoid culture medium was changed every two to three days. In some experiments, the medium was supplemented with 100 ng/ml human Wnt3a (Peprotech), 2  $\mu$ M pifithrin (Sigma-Aldrich), 500  $\mu$ M NAC (Sigma-Aldrich), 250 nM sulforaphane (Sigma-Aldrich), 500 nM 4OHT (Sigma-Aldrich), 500 nM chloroquine (Sigma-Aldrich), 50  $\mu$ g/ml MDP, 100  $\mu$ g/ml LPS, 10 ng/ml flagellin, 500 ng/ml PolyI:C, or 10  $\mu$ g/ml LTA (all from InvivoGen).

### **Whole-mount staining and live imaging on organoids**

Before whole-mount staining, 10  $\mu$ M BrdU was added to the culture medium for 16 hours to label proliferating crypt cells. For staining, the medium was washed off with PBS and organoids were fixed by incubation in 4% paraformaldehyde for 30 min at room temperature. The DNA was denatured by incubation in 2 N HCl for 25 minutes, and non-specific antigens were blocked by incubation with 5% goat serum, 1% BSA, and 0.3% TritonX-100 in PBS before the overnight incubation of the organoids at 4°C with primary antibodies diluted in blocking solution. The organoids were then washed in PBS, incubated overnight at room temperature with fluorescent

secondary antibodies and Hoescht stain, washed, and suspended in Vectashield fluorescence mounting medium (Vector), before being flattened between a slide and coverslip for imaging with a Yokogawa CSU-X1 Spinning Disk (Yokogawa, Tokyo, Japan) coupled to a Leica DMI6000B microscope (Leica Microsystems GmbH, Wetzlar, Germany). For CellROX staining on live organoids, 10  $\mu$ M CellROX™ deep red reagent (Thermo Fisher Scientific) was added to the culture medium and organoids were incubated for 30 min at 37°C, washed in PBS and imaged directly on a Zeiss Axiovert 200M inverted microscope. Hoechst 33342 (Thermo Fisher Scientific) was used to label the nuclei of all cells. Images were then acquired with MetaMorph 7 software.

### **Cell sorting and flow cytometry**

Isolated crypts (as described above) were dissociated by incubation in dispase buffer containing 0.3 U/ml dispase (Corning), 0.8 U/ml DNase (Ambion), 10  $\mu$ M Y-27632 (Enzo) at 37°C for 30 min. Dissociated cells were passed through a cell strainer with 40  $\mu$ m pores (BD Bioscience) centrifuged for 5 min at 700 x *g* and washed with PBS. Cells were stained by incubation with APC-conjugated anti-CD24 antibody (clone M1/69, BioLegend) and PE-Epcam (clone G8.8 BioLegend) for 20 min at 4°C. For RNA extraction, cells were sorted on a BD FACSAria III cell sorter (BD Biosciences) and collected directly in lysis buffer. For the analysis of reactive oxygen species, cells were incubated with 5  $\mu$ M CellROX™ deep red, 5  $\mu$ M MitoSOX™ red, or 250 nM MitoTracker™ deep red reagent (all from Thermo Fisher Scientific) for 20 min at 37°C and washed in PBS before analysis on a BD LSRFortessa™ flow cytometer (BD Biosciences) with BD FACSDIVA™ software (BD Biosciences). Viable single epithelial cells were gated on the basis of forward scatter, side scatter and pulse-width parameters, and were identified on the basis of negative staining with propidium iodide (ThermoFisher Scientific) or with the Live/Dead™ Blue Dead Cell Stain Kit (Thermo Fisher Scientific).

### **Quantitative PCR and microarray analysis**

Total RNA was isolated from cells and tissues in Trizol reagent (Invitrogen), according to the manufacturer's protocol. For RT-qPCR, total RNA was reverse-transcribed with the Maxima First-Strand cDNA Synthesis Kit (Thermo Fisher Scientific). For microarray and RT-qPCR experiments

on sorted Lgr5<sup>+</sup>ISC and TA cells, cells were sorted directly into lysis buffer and RNA was extracted with the RNeasy Micro Kit, according to the manufacturer's instructions (Qiagen). RNA quality was checked with a Bioanalyzer 2100 (with the Agilent RNA6000 nano chip kit), and 500 pg of total RNA was reverse transcribed with the Ovation Pico System V2 (Nugen). The resulting double-stranded cDNA was used for amplification with SPIA technology. Mitochondrial DNA was quantified by subjecting DNA extracted from whole intestinal tissue to qPCR with the LightCycler 480 System and the Luminaris Color HiGreen Kit (Thermo Fisher Scientific). The results are expressed relative to 18s rRNA for all RT-qPCR experiments. Levels of MT-RNR1, which was used to quantify mitochondrial DNA, are expressed relative to RBM15, which was used to quantify nuclear DNA. All primers are listed in supplementary table 1.

For microarray experiments, cDNA amplified from sorted cells was purified according to the Nugen protocol, and 3.6 µg of target sense DNA was fragmented and labeled with biotin, with the Encore Biotin Module kit (Nugen). Fragmentation was checked with the Bioanalyzer 2100, and the cDNA was then hybridized to GeneChip® Mouse Gene 2.0 ST (Affymetrix) at 45°C for 17 hours. Chips were then washed on an FS450 fluidic station, according to the manufacturer's protocols (Affymetrix), and scanned with a GCS3000 7G. The scanned images were then analyzed with Expression Console software (Affymetrix) to obtain raw data (cel files) and metrics for quality control. Data were normalized with the RMA algorithm in Bioconductor, with the custom CDF vs 21 (4). Statistical analysis was performed with Partek® GS 6.6. Differences in gene expression were analyzed by unsupervised hierarchical clustering and PCA, to assess technical bias and identify outlier samples. Two-way ANOVA was used for comparisons between groups by genotype and cell type. We then used an unadjusted *p*-value and the fold-change in expression to filter and select differentially expressed genes. Genes with a *p*-value < 0.05 and a fold-change in expression > 1.2 were considered to be differentially expressed.

### **Western blotting**

Protein extracts were prepared from intestinal tissue or organoids by lysis in Laemmli buffer. Protein extracts were then analyzed by western blotting, as previously described (5). Antibodies against

the following proteins were used: LC3 (Sigma, L7543, 1:1,000), p62 (Enzo, BML-PW9860 1:1,500), ATG7 (Cell Signaling, 2631, 1:1,000), p53 (Leica, NCL-p53-CM5p, 1:200), NRF2 (Cell Signaling, 12721S, 1:400), and  $\gamma$ -tubulin (Sigma-Aldrich, T6557).

### **Electron microscopy**

We fixed 2 mm pieces of tissue in 4% paraformaldehyde and 2% glutaraldehyde in 0.1 M phosphate buffer and stored them at 4°C. The tissues were washed thoroughly several times in 0.1 M phosphate buffer, post-fixed in 1% osmium tetroxide and washed in water before staining with uranyl acetate. The tissues were then embedded in epoxy resin, and 300-400 nm semithin sections were cut to check for the correct orientation of the samples; 80-90 nm sections were then cut on a Reichert Ultracut E ultramicrotome. The ultrathin sections were transferred onto 150-mesh copper grids and stained with uranyl acetate and lead citrate. The sections were then viewed under a JEOL 1011 transmission electron microscope with a GATAN Erlangshen CCD (charge-coupled device) camera.

### **Statistical analysis**

Data are expressed as the mean  $\pm$  SD. Differences were analyzed in unpaired two-tailed Student's *t* tests, with *p*-values < 0.05 considered significant. Detailed *n* values for each panel in the figures are indicated in the corresponding legends. We analyzed a minimum of *n*=3 animals in each case.

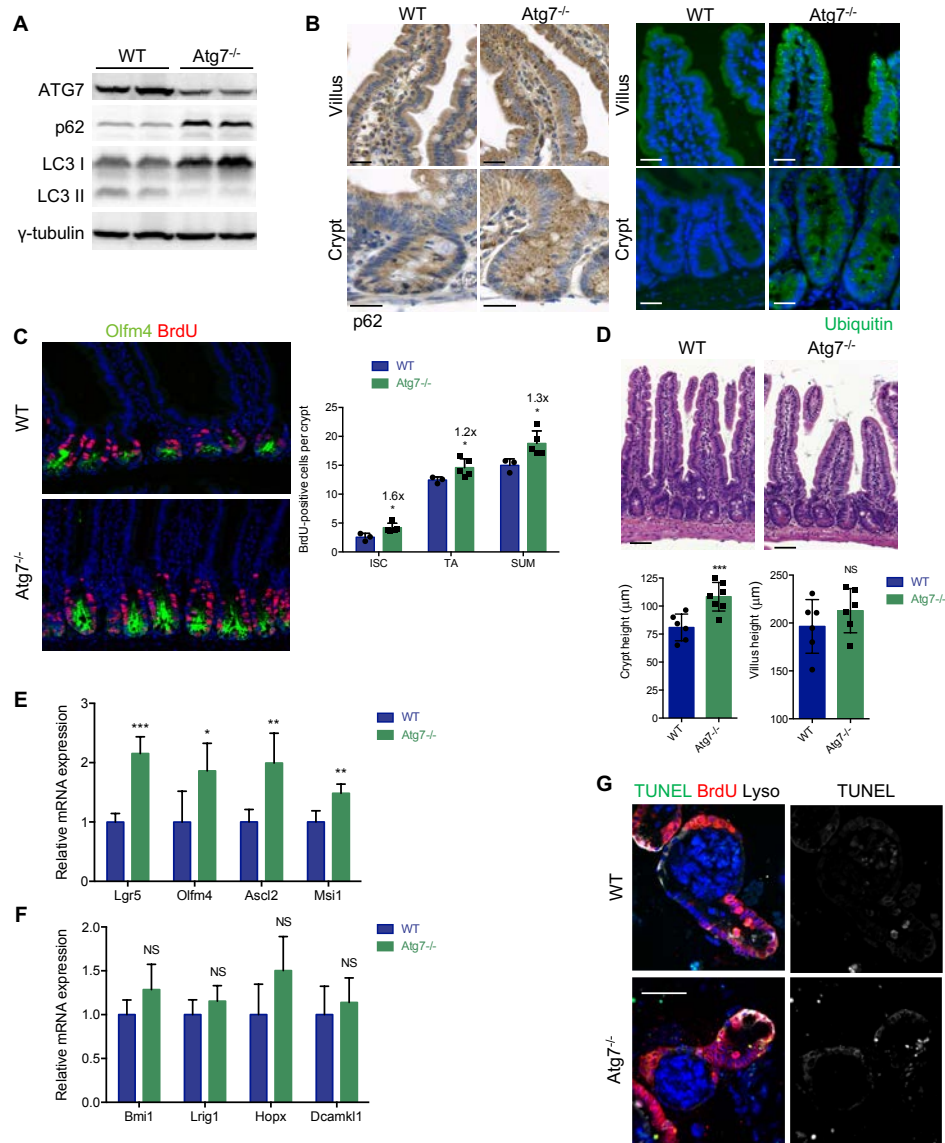


**Fig. S1. Impact of Atg7 deletion on Lgr5<sup>+</sup>ISC pool.** (A) Western blotting for ATG7, p62, and LC3b on whole intestinal tissue lysates from WT and Atg7<sup>-/-</sup> mice.  $\gamma$ -tubulin was used as a loading control. Results are shown for 2 mice of each genotype. (B) Representative staining for p62 and ubiquitin in the crypts and villi of WT and Atg7<sup>-/-</sup> tissue sections. Scale bars: 25  $\mu$ m (C) Representative Olfm4 and BrdU costaining on tissue sections from WT and Atg7<sup>-/-</sup> intestines. Scale bars: 50  $\mu$ m. Quantification of the mean number of BrdU-positive cells per crypt over 50 consecutive whole crypts in 3 WT and 4 Atg7<sup>-/-</sup> mice. The data shown are means  $\pm$  SD. (D) representative HE stainings of WT and Atg7<sup>-/-</sup> tissue sections. Scales bars: 50  $\mu$ m. Quantification of crypt and villus height over 200 sections in 6 WT and 7 Atg7<sup>-/-</sup> mice. (E,F) Relative mRNA levels for genes encoding known markers of Lgr5<sup>+</sup>ISC (E) and reserve or '+4' ISC (F) as assessed by RT-qPCR analysis of whole intestinal tissue lysates from 4 WT and 5 Atg7<sup>-/-</sup> mice. The data shown are means  $\pm$  SD. (G) Representative whole-mount staining of organoids grown from the crypts of WT and Atg7<sup>-/-</sup> mice, 16 hours after the addition of BrdU to the culture medium of organoids. TUNEL staining labels apoptotic cells. Lysozyme staining labels Paneth cells, BrdU staining labels crypt cells. Significant differences: \*  $p < 0.05$ , \*\*  $p < 0.01$ , \*\*\*  $p < 0.005$ . NS: not statistically significant.

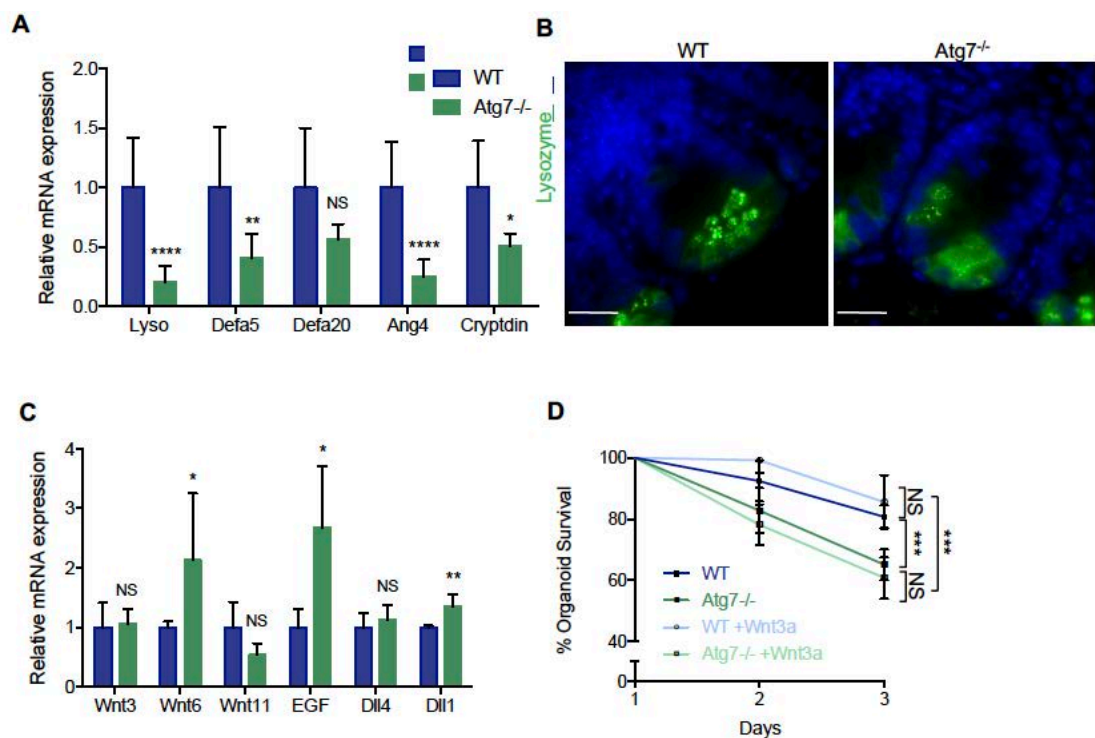


**Fig. S2. Loss of *Atg7* in Paneth cells affects antimicrobial peptides.** (A) Relative mRNA levels for genes encoding antimicrobial peptides produced by Paneth cells, as assessed by RT-qPCR analysis on whole intestinal tissue lysates from 4 WT and 5 *Atg7*<sup>-/-</sup> mice. The data shown are means  $\pm$  SD. Significant differences: \*  $p < 0.05$ , \*\*  $p < 0.01$ , \*\*\*  $p < 0.005$ , \*\*\*\*  $p < 0.001$ . (B) Representative lysozyme staining on tissue sections from WT and *Atg7*<sup>-/-</sup> intestines. Scale bars: 25  $\mu$ m. (C) Relative mRNA levels for genes encoding growth factors produced by Paneth cells, as assessed by RT-qPCR on whole intestinal tissue lysates of 4 WT and 5 *Atg7*<sup>-/-</sup> mice. The data shown are means  $\pm$  SD. (D) Percent survival from day 1 of organoids from the crypts of WT and *Atg7*<sup>-/-</sup> mice in the presence or absence of exogenous Wnt3a in the culture medium ( $n=5$  mice for WT and 7 mice for *Atg7*<sup>-/-</sup>). Significant differences are shown for day 3.



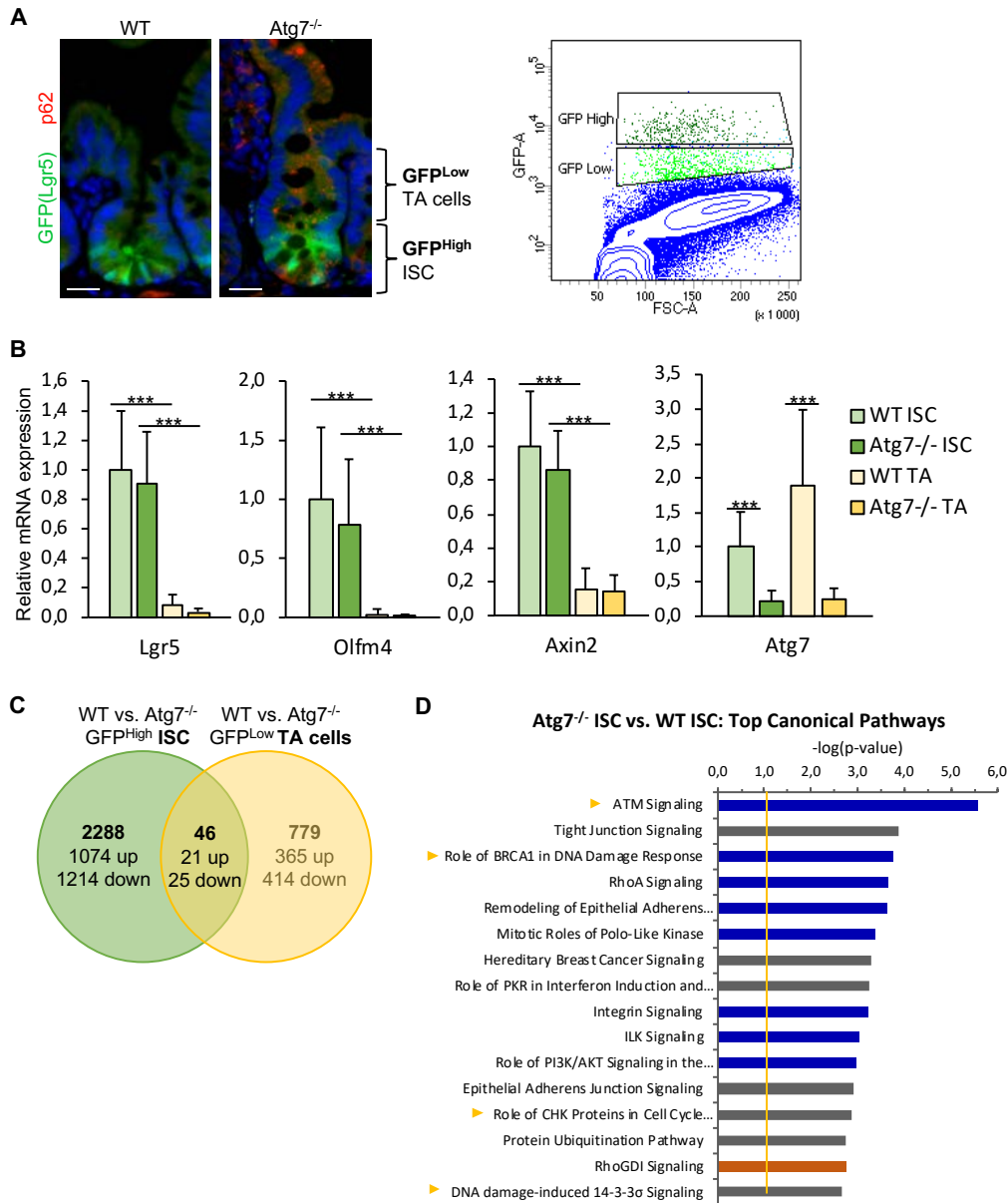


**Fig. S3. Transcriptomic analyses of Atg7 deficiency in Lgr5<sup>+</sup>ISC and progenitors.** (A) Left panel: Representative GFP and p62 costaining on tissue sections from Lgr5WT and Lgr5Atg7<sup>-/-</sup> mice. Hoechst stain was used as a nuclear counterstain. Scale bars: 25  $\mu$ m. Right panel: representative sorting gates for GFP<sup>High</sup> Lgr5<sup>+</sup>ISC and GFP<sup>Low</sup> TA cell populations. (B) Relative mRNA levels, as assessed by RT-qPCR, confirming the stronger expression of Lgr5<sup>+</sup>ISC markers in sorted GFP<sup>High</sup> than in GFP<sup>Low</sup> populations, regardless of genotype, and lower levels of Atg7 in both populations when sorted from Lgr5Atg7<sup>-/-</sup> mice than when sorted from Lgr5WT mice. The data shown are means  $\pm$  SD. ( $n=6-8$  mice per condition). Significant differences: \*  $p<0.05$ , \*\* $p<0.01$ , \*\*\* $p<0.005$ . (C) Summary of genes significantly deregulated in sorted GFP<sup>High</sup> Lgr5<sup>+</sup>ISC or GFP<sup>Low</sup> TA progenitors from Lgr5Atg7<sup>-/-</sup> versus Lgr5WT mice. (D) Top-ranking canonical pathways predicted by Ingenuity Pathway Analysis as significantly deregulated in the transcriptomic signature of sorted GFP<sup>High</sup> Lgr5<sup>+</sup>ISC from the crypts of Lgr5Atg7<sup>-/-</sup> versus Lgr5WT mice. Pathways related to DNA repair are indicated by a yellow arrowhead. Pathways in blue are predicted to be downregulated in ISC from Lgr5Atg7<sup>-/-</sup> mice relative to ISC from Lgr5WT mice, whereas pathways in orange are predicted to be upregulated.

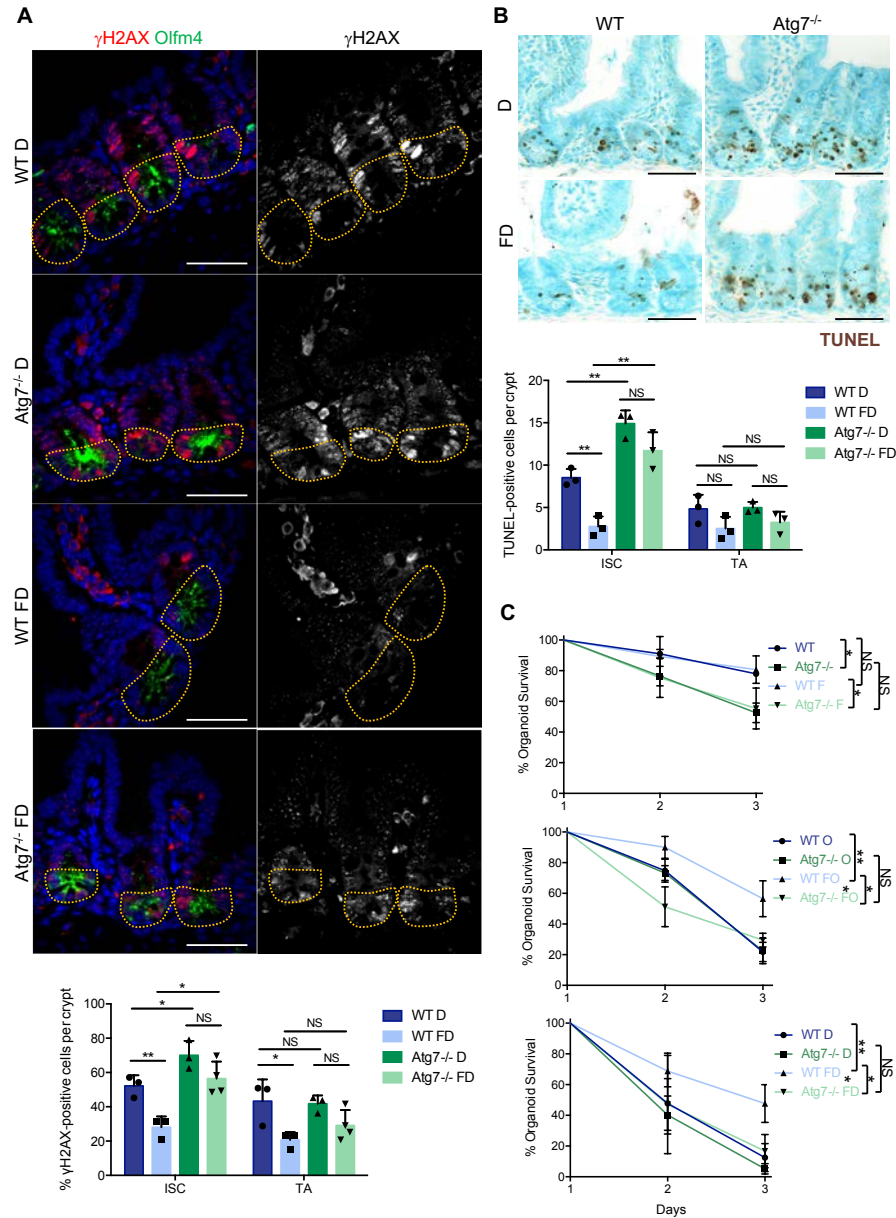


**Fig. S4. Fasting protects *Lgr5*<sup>+</sup>ISC from doxorubicin -induced DNA damage and apoptosis in an *Atg7*-dependent manner.** (A) Representative z-projection (from 20 stacks spanning over 6  $\mu$ m to include whole nuclei) of combined  $\gamma$ H2AX and Olfm4 staining (left) and  $\gamma$ H2AX staining alone (right) in the crypts of WT and *Atg7*<sup>-/-</sup> mice 6 hours after doxorubicin treatment alone (D) or preceded by a 24-hour fast (FD). Scale bars: 50  $\mu$ m. The percentage of  $\gamma$ H2AX-positive cells was determined on at least 10 randomly selected whole crypts per mouse (*n*=3 mice of each genotype). Cells with >4  $\gamma$ H2AX foci in their nuclei were considered  $\gamma$ H2AX-positive. Olfm4<sup>+</sup> cells (circled area) were considered to be ISC and the Olfm4<sup>-</sup> cells above them and below the crypt-villus junction were considered to be TA cells. The data shown are means  $\pm$  SD. (B) Representative TUNEL staining of tissue sections from WT and *Atg7*<sup>-/-</sup> mice 6 hours after doxorubicin treatment alone (D) or preceded by a 24-hour fast (FD). Scale bars: 50  $\mu$ m. Determination of the mean number of TUNEL-positive cells per crypt over 50 consecutive whole crypts in 3 mice per condition. The data shown are means  $\pm$  SD. (C) (Top) Percent survival from day 1 of organoids from the crypts of WT and *Atg7*<sup>-/-</sup> mice either untreated or fasted for 24 hours and then allowed to feed *ad libitum* for 6 hours (F). *n*=2 control mice per genotype and 3 fasted mice per genotype. (Middle) Percent survival from day 1 of organoids from the crypts of WT and *Atg7*<sup>-/-</sup> mice 6 hours after either oxaliplatin treatment

alone (O) or preceded by a 24-hour fast (FO).  $n=4$  mice per condition. (Bottom) Percent survival from day 1 of organoids from the crypts of WT and Atg7<sup>-/-</sup> mice 6 hours after either doxorubicin treatment alone (D) or preceded by a 24-hour fast (FD).  $n=3$  mice per condition. Significant differences are shown for day 3. Significant differences: \*  $p<0.05$ , \*\* $p<0.01$ , \*\*\* $p<0.005$ . NS: not statistically significant.

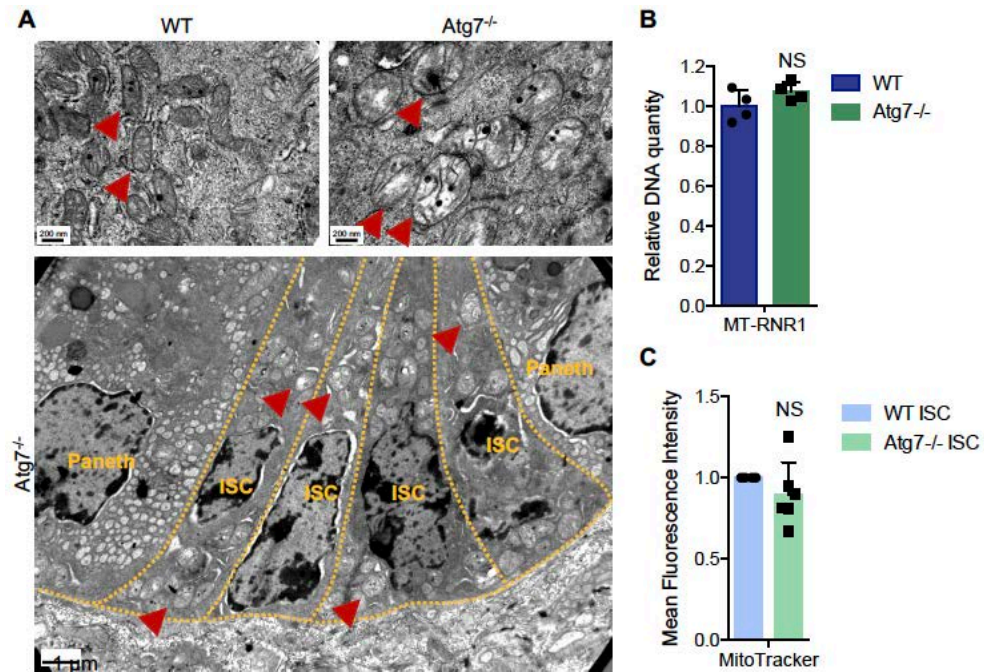


**Fig. S5. Impact of *Atg7* deletion on mitochondria.** (A) Transmission electron microscopy images of intestinal epithelium sections from WT and *Atg7*<sup>-/-</sup> mice, showing mitochondria, indicated by red arrowheads. The bottom panel shows the bottom of an *Atg7*<sup>-/-</sup> crypt, with ISC traced out in yellow and swollen mitochondria in the cytoplasm indicated by red arrowheads. Scale bars: 200 nm for top panels, 1 μm for the bottom panel. (B) Relative mitochondrial DNA quantity, assessed by qPCR analysis of whole intestinal tissue DNA extracts from 4 WT and 4 *Atg7*<sup>-/-</sup> mice. *MT-RNR1* was used to assess mitochondrial DNA content and was normalized against nuclear *RBM15* DNA content. (C) Mean Mitotracker fluorescence intensity of sorted Lgr5<sup>+</sup>ISC from 4 Lgr5<sup>WT</sup> and 6 Lgr5<sup>*Atg7*<sup>-/-</sup></sup> mice. The data shown are means ± SD. NS: not statistically significant.

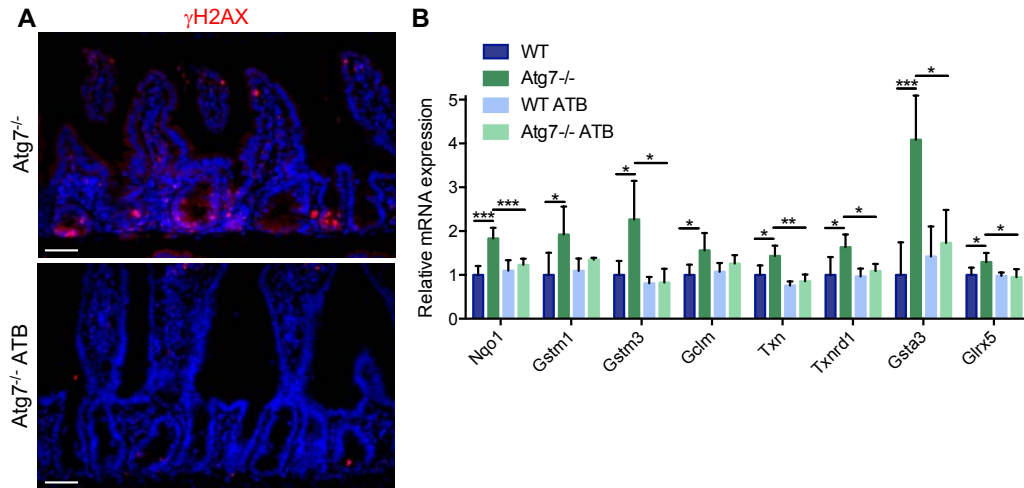


**Fig. S6. Antibiotic treatment decreases DNA damage and antioxidant response gene signature induced by *Atg7* loss.** (A) Representative  $\gamma$ H2AX staining on tissue sections from *Atg7*<sup>-/-</sup> mice treated with water or broad-spectrum antibiotics (ATB). Scale bars: 50  $\mu$ m. (B) Relative mRNA levels for NRF2 target genes encoding antioxidant response proteins, as assessed by RT-qPCR on whole intestinal tissue lysates from 4 control WT, 5 control *Atg7*<sup>-/-</sup>, 5 ATB-treated WT and 3 ATB-treated *Atg7*<sup>-/-</sup> mice. The data shown are means  $\pm$  SD.

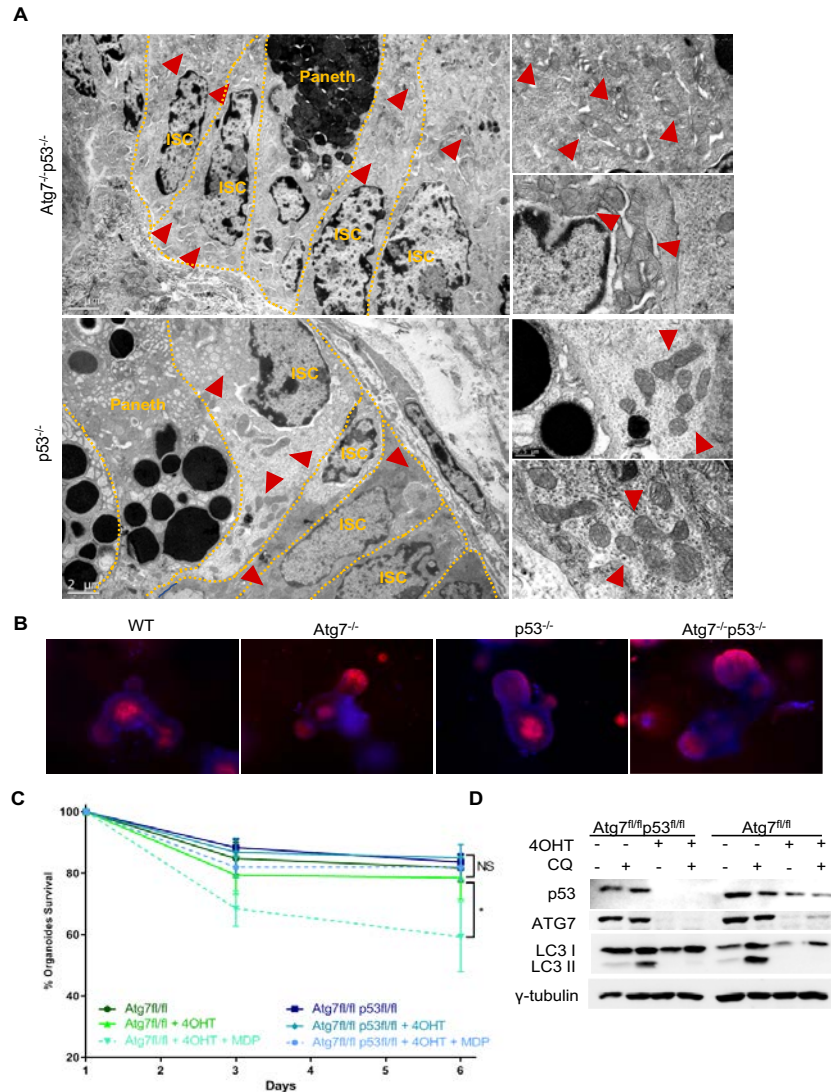


**Fig. S7: Impact of p53 loss on mitochondrial morphology, ROS formation and MDP-associated death following Atg7 deletion.** (A) Transmission electron microscopy images of intestinal epithelium sections from Atg7<sup>-/-</sup>p53<sup>-/-</sup> mice showing accumulation of abnormal mitochondria, indicated by red arrowheads. No alteration of mitochondria is observed in the cytosol of p53<sup>-/-</sup> mice. (B) Representative CellROX staining on live organoids of WT, Atg7<sup>-/-</sup>, p53<sup>-/-</sup> and Atg7<sup>-/-</sup>p53<sup>-/-</sup> mice after 3 days in culture. (C) Percent survival from day 1 of Atg7<sup>fl/fl</sup> and Atg7<sup>fl/fl</sup>p53<sup>fl/fl</sup> organoids in presence or absence of 4OHT and/or MDP in the culture medium ( $n=3$  mice per condition). (D) Western blotting for p53, ATG7 and LC3 on protein extracts from day 6 of Atg7<sup>fl/fl</sup> and Atg7<sup>fl/fl</sup>p53<sup>fl/fl</sup> organoids in the presence or absence of 4OHT and/or CQ in the culture medium.  $\gamma$ -tubulin was used as a loading control.

**Table S1. qPCR primers used in this study**

Gene	F primer	R primer
18S	GTAACCCGTTGAACCCATT	CCATCCAATCGGTAGTAGCG
Ang4	CCCAGTTGGAGGAAAGCTG	CGTAGGAATTTTCGTACCTTTCA
Aslc2	CTACTCGTCGGAGGAAAG	ACTAGACAGCATGGGTAAG
Atg7 (mRNA)	CAGCAGTGATGACCGCATGA	CAAATGCCAGGCTGACAGGA
Atm	TGCAGATTTATATCCATCATCCAC	TTTCATGGATTTCATAAGCACCTT
Axin2	GATTCCCCTTTGACCAGGTGG	CCATTACAAGCAAACCAGAAGT
Bra1	TTCACCAACATGCCCAAAG	AGCTCCTTACCACGGAAG
Cryptdin1	CCAGATCTCTCAACGATTCCTCTT	TTGGAGACCCAGAAGGCACTT
Defa20	CCAGGGGAAGAGGACCAG	TGCAGCGACGTTTTCTACA
Defa5	CAGGCTGATCCTATCCACAAA	GGCCTCAAAGGAGATAGACA
Dll1	GGTTTTCTGTTGCGAGGTCATC	CCCATCCGATTCCCCTTCG
Dll4	TTCCAGGCAACCTTCTCCGA	ACTGCCGCTATTCTTGTC
EGF	TCCTGGACAAACGGCTCTTC	CCTGATAAGACGGACGGAGC
Gclm	TGACTCACAATGACCCGAAA	TCAATGTCAGGGATGCTTTCT
Glx5	CGGGCAGGTGCTTTTACTT	AGTGGTTGTACGTTACCAGAG
Gsta3	GCCTACTTGAGGTACAGCACAAT	AAAGTAATGAAGGACTGGCTTCC
Gstm1	GCAGCTCATGCTCTGTTA	TTTCTCAGGGATGGTCTTCAA
Gstm3	TGAAGGCCATCCCTGAGAAA	CTTGGGAGGAAGCGGCTACT
Lgr5	CCTTGGCCCTGAACAAAATA	ATTTCTTCCAGGGAGTGG
Lyso	GGTCTACAATCGTTGTGAGTTGG	CTCCGAGTTCGGAATATACT
Msi1	GATGCCTTCATGCTGGGTAT	TAGGTGTAACCAGGGGCAAG
Nqo1	AGCGTTCGGTATTACGATCC	AGTACAATCAGGGCTCTTCTCG
Olmf4	GCCACTTCCAATTTTAC	GAGCCTCTTCTCATAAC
Rad51	AAAAACCCATTGGAGGGAAC	CCCCTCTTCTTTCAGG
Reg4	TCCGGAAGCTAAGAACTGG	TGGGATCCATTTCCATATGAC
Txn	TGAAGCTGATCGAGAGCAAG	AGAAGTCCACCACGACAAGC
Txnrd1	CCACATTCACACACGTTCCCT	TTTTGTCACACCGACTCCTCT
Wnt11	CTGCATGAAGAATGAGAAGGTG	ACTGCCGTTGGAAGTCTTGT
Wnt3	CTCGCTGGCTACCCAATTT	GAGGCCAGAGATGTGTACTGC

## References

1. J. Levy *et al.*, Intestinal inhibition of Atg7 prevents tumour initiation through a microbiome-influenced immune response and suppresses tumour growth. *Nat Cell Biol* **17**, 1062-1073 (2015).
2. A. Gregorieff, H. Clevers, In Situ Hybridization to Identify Gut Stem Cells. *Curr Protoc Stem Cell Biol* **34**, 2F 1 1-11 (2015).
3. T. Sato *et al.*, Single Lgr5 stem cells build crypt-villus structures in vitro without a mesenchymal niche. *Nature* **459**, 262-265 (2009).
4. M. Dai *et al.*, Evolving gene/transcript definitions significantly alter the interpretation of GeneChip data. *Nucleic Acids Res* **33**, e175 (2005).
5. G. Peignon *et al.*, Complex interplay between beta-catenin signalling and Notch effectors in intestinal tumorigenesis. *Gut* **60**, 166-176 (2011).